



**HAL**  
open science

## **A prospective comparison of dynamic contrast-enhanced MRI and $^{51}\text{Cr}$ -EDTA clearance for glomerular filtration rate measurement in 42 kidney transplant recipients**

Benjamin Taton, Renaud de La Faille, Julien Asselineau, Paul Perez, Pierre Merville, Thierry Colin, Christian Combe, Steven Sourbron, Nicolas Grenier

### ► **To cite this version:**

Benjamin Taton, Renaud de La Faille, Julien Asselineau, Paul Perez, Pierre Merville, et al.. A prospective comparison of dynamic contrast-enhanced MRI and  $^{51}\text{Cr}$ -EDTA clearance for glomerular filtration rate measurement in 42 kidney transplant recipients. *European Journal of Radiology*, 2019, 117, pp.209-215. 10.1016/j.ejrad.2019.02.002 . hal-02416091

**HAL Id: hal-02416091**

**<https://inria.hal.science/hal-02416091>**

Submitted on 17 Dec 2019

**HAL** is a multi-disciplinary open access archive for the deposit and dissemination of scientific research documents, whether they are published or not. The documents may come from teaching and research institutions in France or abroad, or from public or private research centers.

L'archive ouverte pluridisciplinaire **HAL**, est destinée au dépôt et à la diffusion de documents scientifiques de niveau recherche, publiés ou non, émanant des établissements d'enseignement et de recherche français ou étrangers, des laboratoires publics ou privés.

# A prospective comparison of DCE-MRI and <sup>51</sup>Cr-EDTA for glomerular filtration rate measurement in 42 kidney transplant recipients

---

Benjamin Taton (PhD, MD)<sup>1,2,5</sup>

Renaud De La Faille (MD)<sup>1</sup>

Julien Asselineau (MSc)<sup>3</sup>

Paul Perez (MD, PhD)<sup>3</sup>

Pierre Merville (MD, PhD)<sup>1</sup>

Thierry Colin (PhD)<sup>2,4,5</sup>

Christian Combe (MD, PhD)<sup>1,6</sup>

Steven Sourbron (PhD)<sup>7</sup>

Nicolas Grenier (MD, PhD)<sup>8</sup>

<sup>1</sup> Centre hospitalier universitaire de Bordeaux, Service de néphrologie, transplantation, dialyse – Groupe hospitalier Pellegrin, France.

<sup>2</sup> Univ. Bordeaux, IMB, UMR CNRS 5251, F-33400, Talence, France.

<sup>3</sup> Centre hospitalier universitaire de Bordeaux, pôle de santé publique, unité de soutien méthodologique à la recherche clinique et épidémiologique, France.

<sup>4</sup> Bordeaux INP, IMB, FF-33400 Talence, France.

<sup>5</sup> INRIA Bordeaux Sud-Ouest, MONC team, FF-33400, Talence, France.

<sup>6</sup> Univ. Bordeaux, Unité INSERM 1026, France.

<sup>7</sup> Division of medical physics, University of Leeds, United Kingdom.

<sup>8</sup> Centre hospitalier universitaire de Bordeaux, Service de radiologie et d'imagerie diagnostique et interventionnelle de l'adulte, Groupe hospitalier Pellegrin, France.

## Corresponding author:

Benjamin Taton

E-mail: [benjamin.taton@chu-bordeaux.fr](mailto:benjamin.taton@chu-bordeaux.fr)

Phone: 33 5 56 79 55 38

Fax : 33 5 56 79 61 07

1  
2  
3  
4  
5  
6  
7  
8  
9  
10  
11  
12  
13  
14  
15  
16  
17  
18  
19  
20  
21  
22  
23  
24  
25  
26  
27  
28  
29  
30  
31  
32  
33  
34  
35  
36  
37  
38  
39  
40  
41  
42  
43  
44  
45  
46  
47  
48  
49  
50  
51  
52  
53  
54  
55  
56  
57  
58  
59  
60  
61  
62  
63  
64  
65

# A prospective comparison of dynamic contrast-enhanced MRI and <sup>51</sup>Cr-EDTA clearance for glomerular filtration rate measurement in 42 kidney transplant recipients

---

## Abstract

### Objectives:

To evaluate the performance of dynamic contrast-enhanced MRI measurement of glomerular filtration rate (GFR) compared with the reference standard technique of urinary clearance of <sup>51</sup>Cr-EDTA.

### Patients and methods:

All kidney transplant recipients (KTRs) with an indication for non-urgent contrast-enhanced MRI at our institution were prospectively included between 2008 and 2012. Renographies were acquired by low-dose DCE-MRI then fitted with a two-compartment pharmacokinetic model. MR-GFR was compared with reference isotopic measurements using Bland-Altman diagrams, intraclass correlation coefficient (ICC) and concordance rates.

### Results:

Forty-two KTRs (mean age 51.5 years, 26 – 74) were analyzed. Mean estimated GFR was 48.5±27mL/min/1.73m<sup>2</sup> (24–178 mL/min). The mean bias was +13.2 mL/min (6.4–20.0, +36.9%) ranging from -31.0 mL/min (-41.7%) to +101.4 mL/min (+89.2%) with a

1  
2  
3  
4 large variability (standard-deviation: 22.3 mL/min; limits of agreement: [-30.6 (-43.3—  
5  
6 18.9); +57.0 (45.3–68.7)]). The ICC was 0.32 (0.02–0.56) and the concordance rate was  
7  
8 28.6% (14.9–42.2).  
9

10  
11 **Conclusions:**  
12

13  
14  
15 The large variability of MR-GFR compared with the reference technique precludes its  
16  
17 use in KTRs, whose anatomical peculiarities make standardization of arterial input  
18  
19 function (AIF) difficult.  
20  
21  
22  
23  
24

25 **Keywords:** functional MRI; kidney transplant; glomerular filtration rate; data accuracy.  
26  
27  
28  
29  
30  
31  
32  
33  
34  
35  
36  
37  
38  
39  
40  
41  
42  
43  
44  
45  
46  
47  
48  
49  
50  
51  
52  
53  
54  
55  
56  
57  
58  
59  
60  
61  
62  
63  
64  
65

1  
2  
3  
4  
5  
6  
7  
8  
9  
10  
11  
12  
13  
14  
15  
16  
17  
18  
19  
20  
21  
22  
23  
24  
25  
26  
27  
28  
29  
30  
31  
32  
33  
34  
35  
36  
37  
38  
39  
40  
41  
42  
43  
44  
45  
46  
47  
48  
49  
50  
51  
52  
53  
54  
55  
56  
57  
58  
59  
60  
61  
62  
63  
64  
65

**Abbreviations:**

AIF: arterial input function

DCE-MRI: dynamic contrast-enhanced MRI

Gd-CM: gadolinium based contrast media

GFR: glomerular filtration rate

KTR: kidney transplant recipients

# 1. Introduction

GFR is the hallmark of kidney function in clinical practice. It is generally estimated using formulas that reflect the balance between endogenous synthesis and renal elimination of biological markers (namely creatinine and/or cystatin C) (1). These formulas were built by regression in large specific-population samples. As such, their use to estimate a specific individual's kidney function is often problematic. Measuring the clearance of exogenous markers infused into a patient's bloodstream is considered to be the gold standard for GFR measurement. However, these techniques are not well suited for routine evaluation of kidney function because they are either costly and cumbersome or rely on hypotheses that cannot always be justified. In addition, most often they require nuclear medicine services.

Gadolinium-based contrast media (Gd-CM) have an excellent renal safety profile even in patients with impaired kidney function (2), and have the same pharmacokinetics as the tracers used for clearance measurement techniques (3). Dynamic contrast-enhanced MRI (DCE-MRI) monitors the distribution of Gd-CM in anatomic structures. In association with mathematical models that describe this process, these imaging techniques are promising tools to evaluate kidney function and other physiological parameters of potential interest in nephrology (e.g. renal blood flow, and vascular or tubular transit times). Compared with isotopic methods, MRI provides high-quality anatomic descriptions of the studied organs and as such, it could provide functional maps of native and transplanted kidneys.

Many studies have found encouraging results for native kidneys, in both healthy or diseased (4–11) subjects but biases were highly dependent on both the acquisition

1  
2  
3  
4 protocol and the model used, and error variability was excessively large. Actually, only  
5  
6 Lim (11) achieved performances compatible with a clinical use of the technique.  
7  
8

9  
10 To our knowledge, the case of KTRs has been studied only by Yamamoto *et al.* (12).  
11  
12 These authors focused on the diagnostic value of tubular transit times for acute  
13  
14 rejection, but did not compare MR-GFR with a reference measurement. Investigation of  
15  
16 KTRs offers a rewarding clinical study group because technically they show only slight  
17  
18 respiratory movements, and clinically their follow-up often implies iterative graft biopsies,  
19  
20 making non-invasive procedures highly worthwhile. Moreover, most of them present an  
21  
22 impaired kidney function, and filtration is almost completely performed by the kidney  
23  
24 allograft so that there is no need to determine differential filtration to compare MR-GFR  
25  
26 with reference GFR estimations. This is the first study whose aim was to compare the  
27  
28 performances of DCE-MRI GFR measurements with <sup>51</sup>Cr-EDTA clearance as a  
29  
30 reference technique in KTRs.  
31  
32  
33  
34  
35  
36  
37

## 38 **2. Materials and methods**

### 39 **2.1. Patients**

40  
41  
42  
43  
44  
45 This prospective study was approved by the institutional review board and the  
46  
47 interregional ethics authorities (Comité de protection des personnes Sud-Ouest et  
48  
49 Outre-Mer III), and informed written consent was obtained from all patients. Between  
50  
51 January 2008 and January 2012, all patients with renal transplantation followed in our  
52  
53 department, whose medical condition required a non-urgent contrast-enhanced MRI of  
54  
55 the renal graft, and who had an estimated GFR over 20 mL/min/1.73 m<sup>2</sup> according to the  
56  
57  
58  
59  
60  
61  
62  
63  
64  
65

1  
2  
3  
4 MDRD formula (13), were considered for inclusion to undergo a low-dose MR  
5  
6 renography.  
7

8  
9 Patients with contraindications to MR examinations or isotopic determinations of the  
10  
11 GFR were not included in the study (pregnant or breast-feeding women, patients with  
12  
13 implanted electronic devices, metallic foreign bodies or surgical clips, severe  
14  
15 claustrophobia, known intolerance or allergy to Gd-CM).  
16  
17

18  
19 Demographic data was gathered from the patients' medical records and from electronic  
20  
21 databases. A blood sample was taken to measure creatinemia and hematocrit.  
22  
23 Isotopic GFR measurement and DCE-MRI examination were performed on the same  
24  
25 day to avoid any change in kidney function between measurements.  
26  
27  
28

## 29 30 **2.2. Magnetic resonance imaging** 31

32  
33 MRI images were acquired on a 1.5T MRI scanner (ACS-NT - Philips) using a body  
34  
35 phased-array coil. A three-dimensional saturation-recovery turbo-field echo sequence  
36  
37 was used with the following parameters:  $T_E / T_R = 3.7/6.2\text{ms}$ ;  $\theta = 10^\circ$ ; slice thickness =  
38  
39 10mm, no gap; 5 slices; acquisition matrix  $60 \times 240$ ; reconstructed matrix  $256 \times 256$ ;  
40  
41 approximate voxel size:  $1.6 \times 1.6 \times 10\text{mm}^3$ ; parallel imaging (SENSE method, 1.7  
42  
43 reduction factor). The saturation pulse was applied non-selectively to avoid inflow effects  
44  
45 within the volume. A coronal oblique section was selected to include both the entire  
46  
47 kidney allograft on its long axis and the terminal abdominal aorta within the acquisition  
48  
49 volume, and centered on the renal pedicle. However, in difficult cases, kidney  
50  
51 parenchyma was given priority over the terminal aorta, provided that an arterial signal  
52  
53 remained visible in the acquisition volume.  
54  
55  
56  
57  
58  
59  
60  
61  
62  
63  
64  
65



1  
2  
3  
4 The temporal resolution of the sequence was approximately 2 seconds. Before and after  
5 injection of the contrast agent, images were acquired iteratively 200 times across 6 min  
6  
7 40 s without breath holds; the patient was simply asked to breath slowly. As of the 20th  
8  
9 acquisition, each patient received an intravenous injection of 0.07 mL/kg (33% of a  
10  
11 standard dose) of gadoterate-meglumine (Dotarem®; Guerbet, Roissy, France) with an  
12  
13 infusion rate of 2 mL/s, followed by a 20 mL saline flush at 2 mL/s.  
14  
15  
16  
17  
18

19 In addition to the functional sequence, all subjects underwent standard T1-weighted  
20  
21 gradient echo and T2-weighted fast spin-echo imaging, and 3D contrast-enhanced MR  
22  
23 angiography for morphologic assessment.  
24  
25

### 26 27 **2.2.1. Data analysis**

#### 28 29 *Image processing*

30  
31  
32  
33 Area under the Gd-CM concentration curve (AUC) was computed for each voxel of the  
34  
35 functional acquisition. For each patient, a threshold was manually chosen to identify a  
36  
37 small subset of voxels with the highest AUC in the aorta or the common iliac artery. This  
38  
39 lead to select a region in the center of the terminal aorta, 2-3 pixels away from aortic  
40  
41 boundaries. Quite often, the anatomical configuration made it impossible to acquire both  
42  
43 the graft and the terminal aorta in the same data volume. In such cases, the arterial  
44  
45 region of interest (ROI) was selected in the common iliac artery or in the upper aorta,  
46  
47 depending on the place where the highest AUC were found. The AUC image was also  
48  
49 used to manually delineate the kidney parenchyma (pelvis excluded) on each of the five  
50  
51 slices available for each patient. Motion of the kidney during the acquisition was ignored.  
52  
53  
54  
55  
56  
57  
58 Examples of typical segmentations are shown on Fig. 1.  
59  
60  
61  
62  
63  
64  
65

1  
2  
3  
4 The arterial and renal signals were averaged over the corresponding ROI before being  
5 used as input for the model-fitting algorithm. Signals corresponding to the images and  
6 segmentations given on Fig. 1 are presented as examples on Fig. 2. Kidney volume ( $V$ )  
7 was computed directly from these ROI as the product of a voxel volume by the number  
8 of voxels in the selected region.  
9

10  
11  
12  
13  
14  
15  
16  
17 Image manipulations and delineations were performed offline using a program  
18 developed by (*initials*) using PMI (v. 0.4) and written in IDL (v 6.3).  
19  
20

### 21 *Compartment model*

22  
23  
24  
25 The distribution of Gd-CM in the kidney was described using the compartmental model  
26 proposed by Sourbron *et al.* (9) and depicted on Fig. 3.  
27

28  
29  
30  
31 Gadolinium concentration was assumed to be proportional to the increase of the signal  
32 intensity from the basal situation, denoted  $s_0$ , which was computed from the 20 first  
33 images:  $c(t) \simeq k \times (s(t) - s_0)$ . Coefficient  $k$  is unknown but cancels out in further  
34 computations so that it does not need estimating. The plasma concentration of  
35 gadolinium in the aorta was computed from *full blood* concentration by correcting for the  
36 hematocrit when available. For eleven patients it was not known and was replaced with  
37 the mean value over the whole cohort (35.5%).  
38  
39  
40  
41  
42  
43  
44  
45  
46  
47

48  
49 The 4 parameters of the model (renal plasma flow,  $GFR$ , plasma volume relative to the  
50 kidney volume, tubular mean transit time) were determined by fitting the predicted tissue  
51 concentration with measured data (likelihood maximization using the Levenberg-  
52 Marquardt algorithm (14)). The convergence of the optimization algorithm to a plausible  
53 solution was checked visually by comparing the fitted curve with actual data.  
54  
55  
56  
57  
58  
59  
60  
61  
62  
63  
64  
65

1  
2  
3  
4 Computations were implemented in Python and its associated scientific computing  
5  
6 libraries (15).

### 10 2.2.2. Isotopic GFR measurement

11  
12 Reference GFR values were obtained by measurements of <sup>51</sup>Cr-EDTA renal clearance  
13 (16). A bolus of 100 µCi (3.7 MBq) <sup>51</sup>Cr-EDTA was injected at t=0. Each patient was  
14  
15 asked to drink 5 mL/kg of water at the beginning of the examination and 90mL at t=60  
16  
17 min and asked to void at t=60 min. Blood samples were taken at t=75, 105, 135 and 165  
18  
19 min to determine the plasma concentrations of <sup>51</sup>Cr-EDTA ( $P_t$ ). Patients were asked to  
20  
21 void at t=90, 120, 150 and 180 min and to drink 90mL water at each of these time point.  
22  
23 The volume of urine and urine concentrations of <sup>51</sup>Cr-EDTA were determined for each of  
24  
25 these samples ( $V_{t_1-t_2}$ ,  $U_{t_1-t_2}$ ).

26  
27 The GFR was determined as the mean of four calculations of the urinary clearance of  
28  
29 <sup>51</sup>Cr- EDTA for each time point:

$$30 \quad GFR = \frac{1}{4} \left( \frac{U_{60-90} \times V_{60-90}}{P_{75}} + \frac{U_{90-120} \times V_{90-120}}{P_{105}} + \frac{U_{120-150} \times V_{120-150}}{P_{135}} + \frac{U_{150-180} \times V_{150-180}}{P_{165}} \right)$$

31  
32  
33 An expert (*initials*) reviewed all these measurements. Patients showing significant  
34  
35 deviations from this protocol or with large discrepancies between the four clearance  
36  
37 measurements (coefficient of variation over 10%) were excluded from the study.  
38  
39

### 40 2.2.3. Statistics

41  
42  
43 MR-GFR and <sup>51</sup>Cr-EDTA-GFR were compared using Bland-Altman diagrams (17–19),  
44  
45 intra-class correlation coefficients (ICC) (20) and concordance rates (namely, the  
46  
47 proportion of patients whose GFR measurements did not differ by more than 5 mL/min  
48  
49  
50

1  
2  
3  
4 between the two techniques). Linear regression and correlation coefficients were given  
5  
6 for comparison with previous works. Normality of error distribution in the Bland-Altman  
7  
8 analysis was tested using Kolmogorov-Smirnov tests.  
9

10  
11 As we expected an ICC greater than 0.8, we calculated the minimum sample size to be  
12  
13 55 to obtain a lower bound of the 95% confidence interval of at least 0.6 (this threshold  
14  
15 is considered to represent good agreement between the investigated techniques) (21).  
16  
17

18  
19 Demographic data are presented as *mean ± standard-deviation* or *median [first; third*  
20  
21 *quartile]* when appropriate. Comparisons of GFR measurement error between  
22  
23 subgroups were performed using Wilcoxon tests. Subgroups were defined depending on  
24  
25 the immunosuppressive regimen, the indication of MRI examinations, and the  
26  
27 abnormalities reported by the radiologist who interpreted the standard morphological  
28  
29 acquisitions.  
30  
31

32  
33 Statistics were computed using the R software (version 3.1.2) and the corresponding  
34  
35 packages (22,23).  
36  
37  
38  
39  
40  
41

### 42 **3. Results**

43  
44

45  
46 Patient selection is shown in the flow diagram in Fig. 4. Sixty-nine patients were initially  
47  
48 included in the study. Twenty-seven were excluded because MR renography was not  
49  
50 interpretable (MRI artefacts or poor positioning of the acquisition volume resulting in  
51  
52 sequences without dependable arterial signal) (15 patients), or because their isotopic-  
53  
54 GFR calculation was untrustworthy (12 patients). Finally, 42 patients were analysed (29  
55  
56 men, 13 women; mean age 51.5 years; age range 26—74) (Table 1). The median time  
57  
58  
59  
60  
61  
62  
63  
64  
65

1  
2  
3  
4 from kidney transplantation to isotopic measurements and MRI examination was  
5  
6 397 [113; 1145] days.  
7  
8

9  
10 For most patients, acquiring both the entire kidney and the terminal abdominal aorta at  
11  
12 the same time proved impossible and arterial ROI had to be selected in the upper aorta  
13  
14 or in the common iliac artery: the ROI was taken in the aorta for 35/42 (83.3%) patients,  
15  
16 and in the iliac artery for 7/42 (16.7%) patients. The size of the arterial ROI was on  
17  
18 average  $62 \pm 28$  voxels (median: 54.5, range: 23—154) for the aortic region, and  
19  
20  $8878 \pm 2318$  voxels (median: 8089.5, range: 5617—15262) for the kidney parenchyma  
21  
22 (average volume of the kidney:  $203 \pm 50$  mL; median: 192; range: 135—321).  
23  
24  
25  
26

27  
28 Mean estimated GFR (MDRD formula) of our patients was  $48.5 \pm 27$  mL/min/ $1.73\text{m}^2$   
29  
30 (eGFR range: from 24 to 178). Mean GFR measured by the isotopic reference technique  
31  
32 was  $41.8 \pm 14.5$  mL/min (EDTA-GFR range: from 18.3 to 81.1). Mean GFR measured by  
33  
34 DCE-MRI was  $55.0 \pm 26.0$  mL/min (MR-GFR range: from 23.9 to 170.1 mL/min). As  
35  
36 plasma samples were available, we also determined the plasma clearance of  $^{51}\text{Cr}$ -EDTA  
37  
38 according to Bröchner-Mortensen's technique (24) as an alternative reference  
39  
40 measurement. As already stated in previous works (25), the two techniques were in  
41  
42 good agreement, plasma clearance being slightly higher than renal clearance (mean  
43  
44 difference between measurements:  $4.3 \pm 7.6$  mL/min). The use of either reference  
45  
46 technique did not change the conclusion of our study (see supplemental material Fig. S3  
47  
48 and S4).  
49  
50  
51  
52  
53

54  
55  
56 The comparison between MR-GFR and the reference method is depicted in Fig. 5.  
57  
58 There was a fair correlation between both measurements ( $p < 0.001$ ,  $r = 0.52$ ). The  
59  
60  
61  
62  
63  
64  
65

1  
2  
3  
4 regression line of MR-GFR against EDTA-GFR had a slope of 0.92 and an intercept  
5  
6 of 16.5 mL/min. Our measurement protocol lead to a large overestimation of the GFR  
7  
8 compared with the reference technique. The mean difference with the reference  
9  
10 technique was  $+13.2 \pm 22.3$  mL/min (6.4—20.0, +36.9%) with a large variability (limits of  
11  
12 agreement: [-30.6(-42.3—18.9); 57.0(45.3—68.7)]). The ICC was 0.32 (0.02—0.56), far  
13  
14 below the 0.6 threshold for satisfactory agreement between the two techniques. The  
15  
16 concordance rate was 28.6% (14.9—42.2). Finally, on average, the systematic bias was  
17  
18 slightly increasing with the GFR value (+0.28 mL/min per mL/min increase).  
19  
20  
21  
22  
23

24  
25 When comparing subgroups of patients depending on their immunosuppressive  
26  
27 regimen, the indication for the MRI, or the morphological abnormalities, no specific  
28  
29 characteristic presented a significant association with larger measurement errors  
30  
31 (Fig. 6).  
32  
33

34  
35 To investigate the influence of ROI selection on measured GFR, we restricted our  
36  
37 analysis to the patients for whom the AIF could be determined from the aorta (36/42,  
38  
39 86% of patients). In these patients, the mean bias was  $11.6 \pm 18.3$  mL/min, with  
40  
41 [-24.2(-34.6—13.8); +47.6(37—57.8)] limits of agreement (vs.  $13.2 \pm 22.3$  mL/min in the  
42  
43 whole cohort). The decrease in error variability was not statistically significant ( $p=0.38$   
44  
45 for the modified one-sided paired Pitman-Morgan test). In a second experiment the AIF  
46  
47 was determined from the iliac artery in a region as close as possible of the implantation  
48  
49 of the kidney allograft artery and the GFR was computed using this new AIF (this was  
50  
51 possible for 37/42 (88%) patients). In comparison with the aortic AIF, the mean bias was  
52  
53  $24.2 \pm 25.5$  mL/min (vs.  $11.6 \pm 18.3$ ) with [-25.8(-40.3—11.3); +74.3(59.8—88.8)] limits of  
54  
55 agreement. The decrease in error variability did not reach statistical significance  
56  
57  
58  
59  
60  
61  
62  
63  
64  
65

1  
2  
3  
4 (p=0.26). The associated Bland-Altman diagrams are presented in the supplemental  
5  
6 material (Fig. S2).  
7  
8  
9

## 10 **4. Discussion**

11  
12  
13  
14  
15 This is the first study performed in a cohort of KTRs for whom non-invasive GFR  
16  
17 measurement would be extremely worthwhile and who show a wide range of GFR  
18  
19 values measured with a reference technique. We chose to exclude all the patients with  
20  
21 doubtful isotopic measurements (12/69) to reinforce the value of this reference  
22  
23 technique, keeping only trustworthy results.  
24  
25  
26

27  
28 Overall, while using DCE-MRI to estimate GFR was feasible for KTRs, compared to the  
29  
30 reference technique, DCE-MRI strongly overestimated GFR and exhibited a large  
31  
32 variability with poor intra-class correlation coefficients and low concordance rates.  
33  
34

35  
36 Whereas there is no other experience in the literature on KTRs for comparison, our  
37  
38 results are somewhat consistent with previously published work on native kidneys but  
39  
40 exhibit a higher systematic bias and larger error variability.  
41  
42

43  
44 Using a Rutland-Patlak technique in 28 diseased subjects, Hackstein *et al.* (5) found a  
45  
46 correlation coefficient  $r=0.86$  between iopromide clearance measurements and MR-  
47  
48 GFR, and a standard deviation from the regression line of 14.8 mL/min. In 39 patients  
49  
50 with a large range of GFR, Buckley *et al.* (6) also found a strong correlation between  
51  
52 isotopic reference measurements and MR-GFR (Spearman's  $\rho$ : 0.81). In another  
53  
54 population of diseased subjects, using and slightly different pharmacokinetic models but  
55  
56 the same acquisition protocol, Lee *et al.* (7) and Zhang *et al.* (8) obtained consistent  
57  
58  
59  
60  
61  
62  
63  
64  
65

1  
2  
3  
4 results: mean bias of -11.8 and -18.1 mL/min, and variability of  $\pm 13.7$  and  $\pm 13.9$  mL/min  
5  
6 respectively in comparison with isotopic GFR determination (correlation coefficient was  
7  
8  $r=0.82$ ). In the same population, with the same acquisition protocol and reference  
9  
10 technique but with 8 different pharmacokinetic models, Bokacheva *et al.* (9) also found a  
11  
12 good correlation between MR-GFR and reference measurements (correlation  
13  
14 coefficients ranging from 0.74 to 0.85). Nonetheless, biases were highly dependent on  
15  
16 the model used, ranging from -52% to -2.5%. Vivier *et al.* (11) experimented other  
17  
18 acquisition and post-treatment protocols with variants of the pharmacokinetic model by  
19  
20 Zhang *et al.* in 20 patients with cirrhosis. Depending on the variant of the model and the  
21  
22 orientation of the slice used for the post-processing, they found a median bias ranging  
23  
24 from -7.7 to -4.1 mL/min, with a root mean square error between 12.8 and 12.9 mL/min.  
25  
26 The most promising results were obtained by Lim *et al.* in diseased patients with a wide  
27  
28 range of GFR (12). Compared with reference isotopic GFR measurements, their protocol  
29  
30 achieved a non-significant mean bias of -0.7 mL/min and variability of  $\pm 5.86$  mL/min,  
31  
32 small enough to be compatible with clinical use.  
33  
34  
35  
36  
37  
38  
39  
40

41 Discrepancies of our results with previous works could be explained both by anatomic  
42  
43 characteristics of transplanted kidneys compared to natives ones and by our workflow  
44  
45 with respect to these characteristics.  
46  
47

48  
49 In term of anatomic characteristics, in contrast with native kidneys, renal allografts  
50  
51 exhibit a large variability in their anatomical configurations. This problem, which has  
52  
53 been highly underestimated, made very difficult to combine an accurate positioning of  
54  
55 the acquisition slab along the long axis of the graft and inclusion of the terminal aorta or  
56  
57 of the common iliac artery. As illustrated on Fig. 2, this resulted in difficulties to achieve  
58  
59  
60  
61  
62  
63  
64  
65



1  
2  
3  
4 standardized and reproducible ROIs selection for the AIF. The 10mm thick coronal slices  
5  
6 also favoured partial volume effects (PVE), mainly when AIF had to be sampled on iliac  
7  
8 arteries instead of aorta, resulting in an underestimation of the AIF, and subsequently, in  
9  
10 an overestimation of GFR. As the importance of PVE depends on the position of the  
11  
12 acquisition matrix with respect to the arteries, which cannot be controlled, this probably  
13  
14 accounts for a large part of the higher variability we noticed compared with  
15  
16 measurements on native kidneys. The increase in the bias noticed when using an AIF  
17  
18 sampled from the iliac arteries (see supplemental material, Fig. 4), which are more  
19  
20 prone to PVE due to their smaller diameter, is consistent with this hypothesis. Finally,  
21  
22 the close proximity of renal parenchyma with iliac vessels could also produce PVE,  
23  
24 mixing signals coming from both structures.  
25  
26  
27  
28  
29  
30

31  
32 Considering the model of Gd-CM pharmacokinetics, the interstitial compartment induces  
33  
34 large overestimation of GFR. This hypothesis is consistent with the results obtained in  
35  
36 most previous studies since the most negative biases are noticed mostly in the patients  
37  
38 with the highest reference GFR measurements. In our cohort, most patients had an  
39  
40 impaired kidney function, a setting often associated with fibrosis in KTRs, which could  
41  
42 explain the observed positive bias. However, no histological evaluation of the interstitial  
43  
44 volume was performed, and this hypothesis remains speculative.  
45  
46  
47  
48

49  
50 Also, in our population of KTRs, the whole filtration function was attributed the  
51  
52 transplant. However, some patients actually have a residual function from their native  
53  
54 kidneys that presumably ranges from 0 to 10 mL/min. While this hypothesis is not  
55  
56 consistent with GFR overestimation, it cannot be ruled out and may explain part of the  
57  
58 large variability we noticed.  
59  
60  
61  
62  
63  
64  
65

1  
2  
3  
4 At last, kidney motion was ignored because transplants are located far away from the  
5  
6 diaphragm muscle. However spontaneous voluntary or digestive motions actually  
7  
8 occurred and have inescapably increased error variability. This suggests that, even for  
9  
10 KTRs, motion correction could prove beneficial to obtain reproducible results.  
11  
12  
13  
14

## 15 **5. Conclusion**

16  
17  
18  
19 This first study on the performance of MR-measurement of GFR in KTRs with respect to  
20  
21 a reference technique shows that, even if kidney grafts are unique, less mobile and  
22  
23 more superficially located, an overestimation and a large variability still precludes its use  
24  
25 in clinical practice without significant improvements. Anatomical constraints make the  
26  
27 standardization of ROI selection more difficult than in native kidneys and lead to larger  
28  
29 and unpredictable partial volume effects. These characteristics hamper an accurate and  
30  
31 reproducible measurement of AIF and probably contribute for a large part to bias and  
32  
33 variability.  
34  
35  
36  
37  
38  
39  
40

## 41 **6. Acknowledgements**

42  
43  
44  
45 Blinded for submission.  
46  
47  
48  
49

## 50 **References**

- 51  
52  
53  
54 1. Levey A, Inker L, Coresh J. GFR estimation: from physiology to public health. *Am*  
55 *J Kidney Dis.* 2014;63:820–834.  
56  
57 2. Soyer P, Dohan A, Patkar D, Gottschalk A. Observational study on the safety  
58 profile of gadoterate meglumine in 35,499 patients: the SECURE study. *J Magn Reson*  
59 *Imaging.* 2017;45(4):988–997.  
60  
61  
62  
63  
64  
65

3. Choyke P, Austin H, Frank J, Girton M, Diggs R, Dwyer A, et al. Hydrated clearance of gadolinium-DTPA as a measurement of glomerular filtration rate. *Kid Int.* 1992;41:1595–1598.
4. Hackstein N, Heckrodt J, Rau W. Measurement of single-kidney glomerular filtration rate using a contrast-enhanced dynamic gradient-echo sequence and the Rutland-Patlak plot technique. *J Magn Reson Im.* 2003;18:714–725.
5. Buckley D, Shurrab A, Cheung C, Jones A, Mamtora H, Kalra P. Measurement of single kidney function using dynamic contrast-enhanced MRI: comparison of two models in human subjects. *J Mag Reson Imaging.* 2006;1117–1123.
6. Lee V, Rusinek H, Bokacheva L, Huang A, Oesingmann N, Chen Q, et al. Renal function measurements from MR renography and a simplified multicompartment model. *Am J Physiol Ren Physiol.* 2007 May;292:F1548–F1559.
7. Zhang J, Rusinek H, Bokacheva L, Lerman L, Chen Q, Prince C, et al. Functional assessment of the kidney from magnetic resonance and computed tomography renography: impulse retention approach to a multicompartmental model. *Magn Reson Med.* 2008 Feb;59(2):278–288.
8. Bokacheva L, Rusinek H, Zhang J, Chen Q, Lee V. Estimates of glomerular filtration rate from MR renography and tracer kinetics models. *J Magn Reson Imaging.* 2009;29:371–382.
9. Sourbron S, Michaely H, Reiser M, SO S. MRI-measurement of perfusion and glomerular filtration in the human kidney with a separable compartment model. *Invest Radiol.* 2008 Jan;43(1):40–48.
10. Vivier P, Storey P, Rusinek H, Zhang J, Yamamoto A, Tantillo K, et al. Kidney function: glomerular filtration rage measurement with MR renography in patients with cirrhosis. *Radiology.* 2011;259(2):462–470.
11. Lim S, Chrysochou C, Buckley D, Kalra P, Sourbron S. Prediction and assessment of responses to renal artery revascularization with dynamic contrast-enhanced magnetic resonance imaging: a pilot study. *Am J Physiol Ren Physiol.* 2013;305(5):F672–F678.
12. Yamamoto A, Zhang J, Rusinek H, Chandarana H, Vivier P, Babb J, et al. Quantitative evaluation of acute renal transplant dysfunction with low-dose three dimensional MR renography. *Radiology.* 2011;260(3):781–789.
13. Lenihan C, O’Kelly P, Mohan P, Little D, Walshe J, Kieran N, et al. MDRD-estimated GFR at one year post-renal transplant is a predictor of long-term graft function. *Ren Fail.* 2008;30:345–352.
14. Press W, Teukolsky S, Vetterling W, Flannery B. Numerical recipes: the art of scientific computing. In Cambridge University Press; 2007. p. 773–839.
15. Jones E, Oliphant T, Peterson P, others. SciPy: Open source scientific tools for Python [Internet]. 2001. Available from: <http://www.scipy.org/>
16. Soveri I, Berg U, Björk J, Elinder C, Grubb A, Mejare I, et al. Measuring GFR: a systematic review. *Am J Kid Dis.* 2014;64(3):411–424.

1  
2  
3  
4 17. Bland J, Altman D. Statistical methods for assessing agreement between two  
5 methods of clinical measurement. *Lancet*. 1986 Feb;307–310.  
6  
7 18. Hamilton C, Stamey J. Using Bland-Altman to assess agreement between two  
8 medical devices – don't forget the confidence intervals! *J Clin Monit Comput*.  
9 2007;21(6):331–333.  
10  
11 19. Euser A, Dekker F, le Cessie S. A practical approach to Bland-Altman plots and  
12 variation coefficients for log-transformed variables. *J Clin Epidemiol*. 2008;61(10):978–  
13 982.  
14  
15 20. Bartko J. The intraclass correlation coefficient as a measure of reliability. *Physiol*  
16 *Rep*. 1966;19:3–11.  
17  
18 21. Bonett D. Sample size requirements for estimating intraclass correlations with  
19 desired precision. *Stat Med*. 2002;21:1331–1335.  
20  
21 22. Team RC. R: A language and environment for statistical computing [Internet].  
22 Vienna, Austria: R Foundation for Statistical Computing; 2013. Available from:  
23 <http://www.R-project.org>  
24  
25 23. Gamer M, Lemon J, Fellows I, Singh P. irr: various coefficients of interrater  
26 reliability and agreement [Internet]. 2012. Available from: [http://CRAN.R-](http://CRAN.R-project.org/package=irr)  
27 [project.org/package=irr](http://CRAN.R-project.org/package=irr)  
28  
29 24. Bröchner-Mortensen J. A simple method for the determination of glomerular  
30 filtration rate. *Scand J Clin Lab Invest*. 1972;30:271–274.  
31  
32 25. Moore A, Park-Holohan S, Blake G, Fogelman I. Conventional measurements of  
33 GFR using 51Cr-EDTA overestimate true renal clearance by 10 percent. *Eur J Nucl*  
34 *Med*. 2003;30(1):4–8.  
35  
36  
37  
38  
39

40 **Tab. 1. Demographic characteristics of the 42 kidney-transplant recipients**  
41 **and 34 donors analyzed.** The number of patients for which the data were available is  
42 given in the third column (*n*).  
43  
44  
45  
46  
47  
48  
49  
50  
51  
52  
53  
54  
55  
56  
57  
58  
59  
60  
61  
62  
63  
64  
65

1  
2  
3  
4 **Fig. 1. Examples of manual delineations of arterial and parenchymal region of**  
5 **interest (red regions) on the AUC images.** Left: case where both the terminal aorta  
6 and the kidney allograft could be included in the same acquisition volume. Isotopic GFR  
7 was 34.4 mL/min, MR-GFR was 60.7 mL/min. Right: case where the anatomical  
8 configuration made this impossible. In this case, the distinction between the common  
9 iliac aorta and the allograft parenchyma is very difficult, due to anatomical proximity and  
10 partial volume effects (white arrows). Isotopic GFR was 81.1 mL/min, MR-GFR was 69.4  
11 mL/min.  
12  
13

14  
15 **Fig. 2. Gadolinium concentration time curves in the blood (red, solid), the allograft**  
16 **parenchyma (black, dashed), and predicted by the model with the optimal**  
17 **parameters (purple, dash-dotted).** The presented signals correspond to the mean  
18 value of the corresponding ROIs, as presented on Fig. 1. Left (top), and Fig. 1. Right  
19 (bottom).  
20  
21

22  
23 **Fig. 3. Pharmacokinetic model used in the study.** Gadolinium enters the vascular  
24 compartment (denoted  $p$ , with a volume  $v_p$ ) with arterial plasma with a flow that  
25 corresponds to the renal plasmatic flow ( $RPF$ ) and a concentration  $c_A(t)$ . Part of it is  
26 filtered into a tubular compartment (denoted  $e$ , with a volume  $v_e$ ) with a coefficient that  
27 corresponds to the glomerular filtration rate ( $GFR$ ). The remaining ( $RPF - GFR$ ) is  
28 returned to the general circulation. The filtered gadolinium is subsequently eliminated  
29 into the bladder with a transit time that is a parameter of the model. The dashed line  
30 represents reabsorption of gadolinium-free fluid.  
31  
32

33  
34 **Fig. 4. Flow-chart of the study.** Twelve patients were excluded because their  
35 reference measurement was not reliable (large discrepancies between the four  
36 measurements of the renal clearance of  $^{51}\text{Cr-EDTA}$ ). Fifteen patients were excluded  
37 because the MRI acquisition was not suitable for GFR measurements (MRI artifacts, bad  
38 positioning of the acquisition volume).  
39  
40

41  
42 **Fig. 5. Relationship between MR-GFR and the reference measurements.** Top-left:  
43 linear regression of MR-GFR against  $^{51}\text{Cr-EDTA}$  clearance: slope was 0.92, intercept  
44 was 16.5 mL/min, correlation coefficient was 0.52. The regression line is plotted with a  
45 solid line. The (ideal) identity line is plotted with a dashed line. Each point corresponds  
46 to one the measurements for one patient. Top-right: Bland-Altman diagram. The dashed  
47 line represents the mean bias over the whole cohort (+13.2 mL/min). Dotted lines  
48 represent the limits of agreement ([-30.6; +57.0]). Normality of errors was tested using a  
49 Kolmogorov-Smirnov test ( $p = 0.21$ ). The ideal no-difference line is draw with a solid  
50 line. Each point corresponds to the measurement for one patient. Bottom-left: Bland-  
51 Altman analysis with log-transformed data (Kolmogorov-Smirnov test:  $p = 0.90$ ). Bottom-  
52 right: limit of agreement computed from Bland-Altman analysis of the log-transformed  
53 data. On average, the systematic bias is slightly increasing with the GFR (+0.28 mL/min  
54 per mL/min increase). The dashed line corresponds to the mean ratio between the bias  
55 and the mean of EDTA clearance and MR-GFR. The dotted lines correspond to the limit  
56 of agreements of the ratio, as depicted in the bottom-left figure.  
57  
58  
59  
60  
61  
62  
63  
64  
65

1  
2  
3  
4  
5  
6  
7  
8  
9  
10  
11  
12  
13  
14  
15  
16  
17  
18  
19  
20  
21  
22  
23  
24  
25  
26  
27  
28  
29  
30  
31  
32  
33  
34  
35  
36  
37  
38  
39  
40  
41  
42  
43  
44  
45  
46  
47  
48  
49  
50  
51  
52  
53  
54  
55  
56  
57  
58  
59  
60  
61  
62  
63  
64  
65

**Fig. 6. Discrepancies between EDTA clearance and MR-GFR (relative values)** depending on the use of calcineurin inhibitors in the patient's immunosuppressive regimen (Wilcoxon exact test:  $p = 0.32$ ), the indication of the MRI examinations (exact Wilcoxon tests:  $p = 0.08, 0.68, 0.99, 0.42, 0.84$  for hypertension, vascular anomaly, urological anomaly, renal mass and kidney failure respectively), and on the abnormalities reported by the radiologist (Wilcoxon exact test:  $p = 0.85, 0.06, 0.71$  and  $0.08$  for the association with renal artery stenosis, dilation of pelvi-caliceal cavities, perirenal collection and perfusion defect respectively).

## 6. Acknowledgements

This study was supported by a public grant from the French National Research Agency (ANR) within the context of the “Investment for the Future” program, referenced ANR-10-LABX-57 and named TRAIL, the French State managed by the ANR referenced ANR-10-IDEX-03-02, named IdEx Bordeaux CPU, and the Centre Hospitalier Universitaire de Bordeaux (AOI-05). The authors thank Corinne Castermans, for her help in data managing and Pippa McKelvie-Sebileau, MSc, Bordeaux, France, for medical editorial assistance in English.

1  
2  
3  
4  
5  
6  
7  
8  
9  
10  
11  
12  
13  
14  
15  
16  
17  
18  
19  
20  
21  
22  
23  
24  
25  
26  
27  
28  
29  
30  
31  
32  
33  
34  
35  
36  
37  
38  
39  
40  
41  
42  
43  
44  
45  
46  
47  
48  
49  
50  
51  
52  
53  
54  
55  
56  
57  
58  
59  
60  
61  
62  
63  
64  
65

Characteristics	Value	<i>n</i>
Patient		
age (yrs)	51.5±12.9	42
males / females	29 (69.1%) / 13(30.9%)	42
eGFR (mL/min/1.73m <sup>2</sup> )*	48.5±27.0	42
hematocrit (%)	35.5±5.3	31
Kidney donor		
age (yrs)	50.6±16.6	34
males	17 (50%)	34
females	17 (50%)	34
Elapsed time from graft to MRI	397 [113; 1445]	42
Immunosuppressive regimen		
calcineurin inhibitors	37 (88.1%)	42
Indication for MRI examination		
vascular anomaly	24 (57.2%)	42
urologic anomaly	8 (19%)	42
arterial hypertension	3 (7.1%)	42
kidney failure	2 (4.8%)	42
renal mass	2 (4.8%)	42
other	3 (7.1%)	42

\*eGFR according to the MDRD formula

**Tab. 1. Demographic characteristics of the 42 kidney-transplant recipients and 34 donors analyzed.** The number of patients for which the data were available is given in the third column (*n*).



Figure 1  
[Click here to download high resolution image](#)

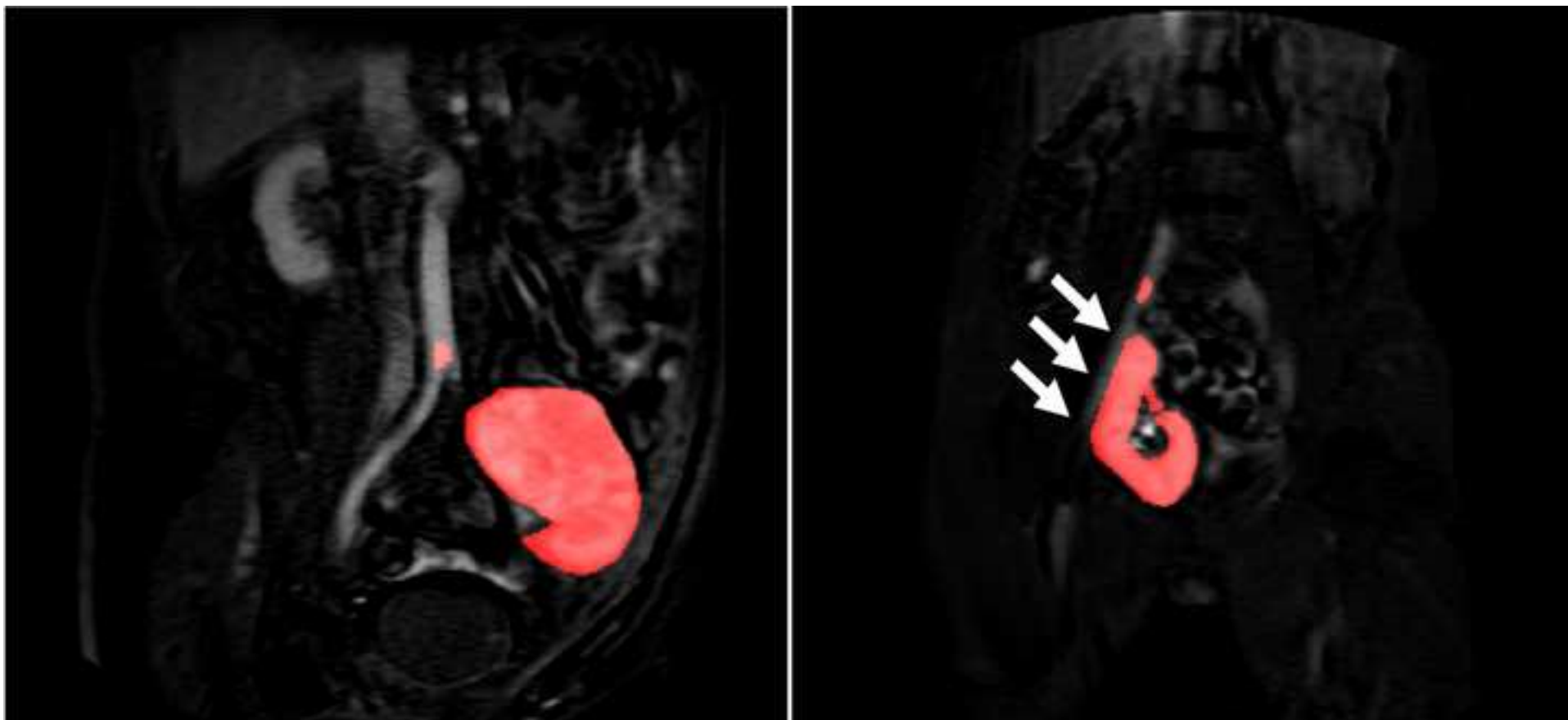


Figure 2

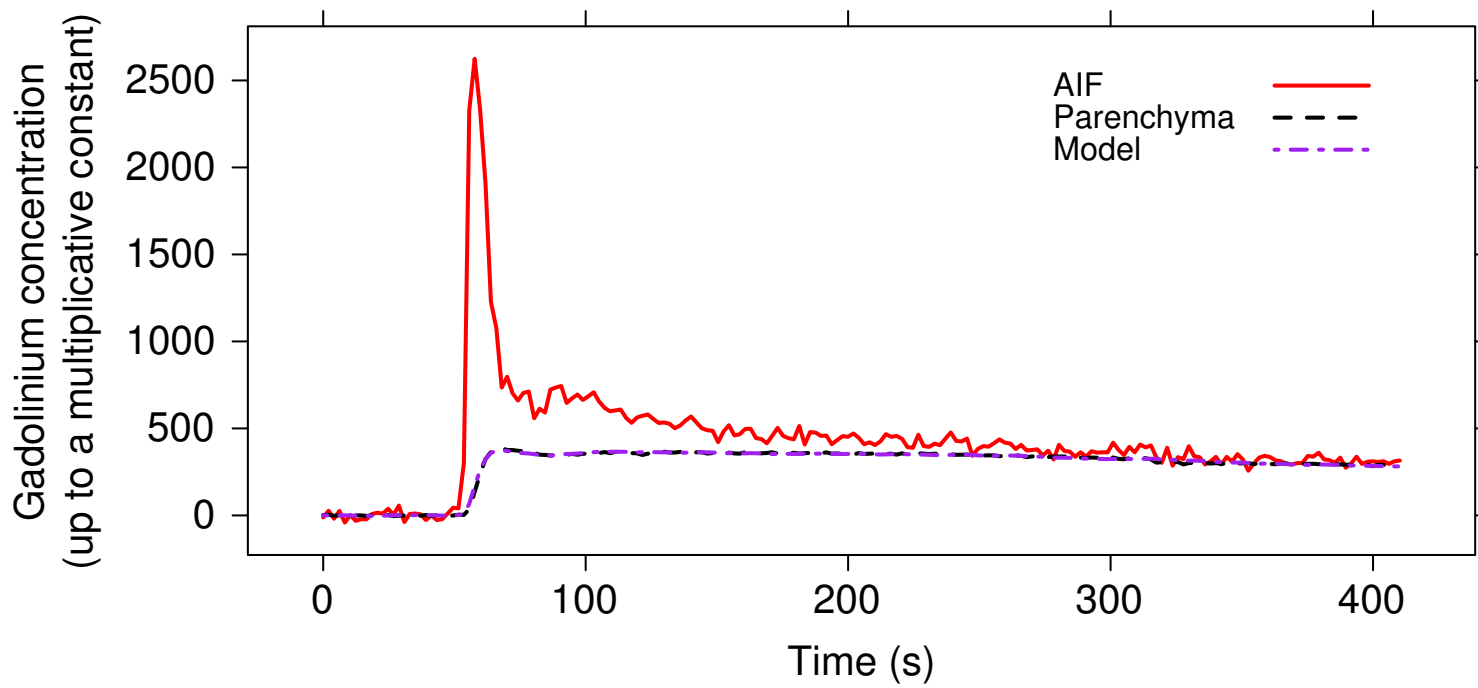
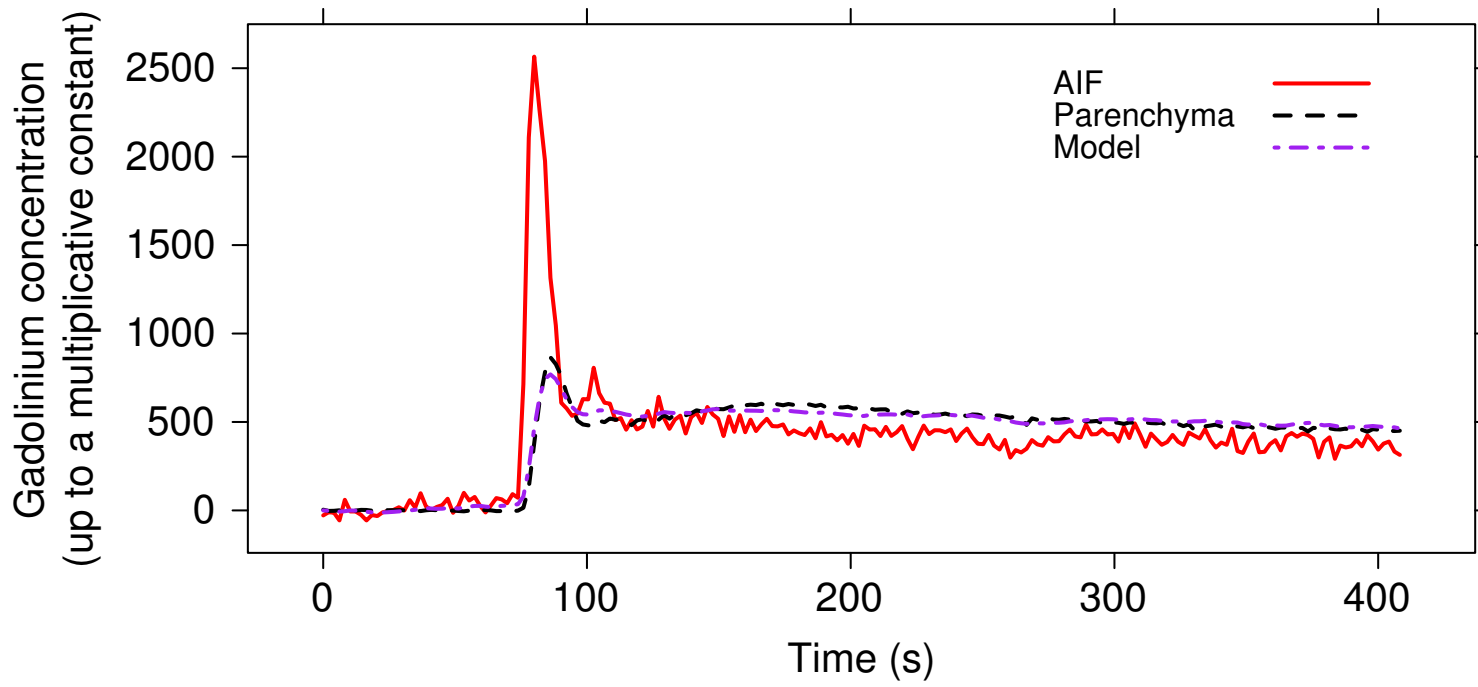


Figure 3

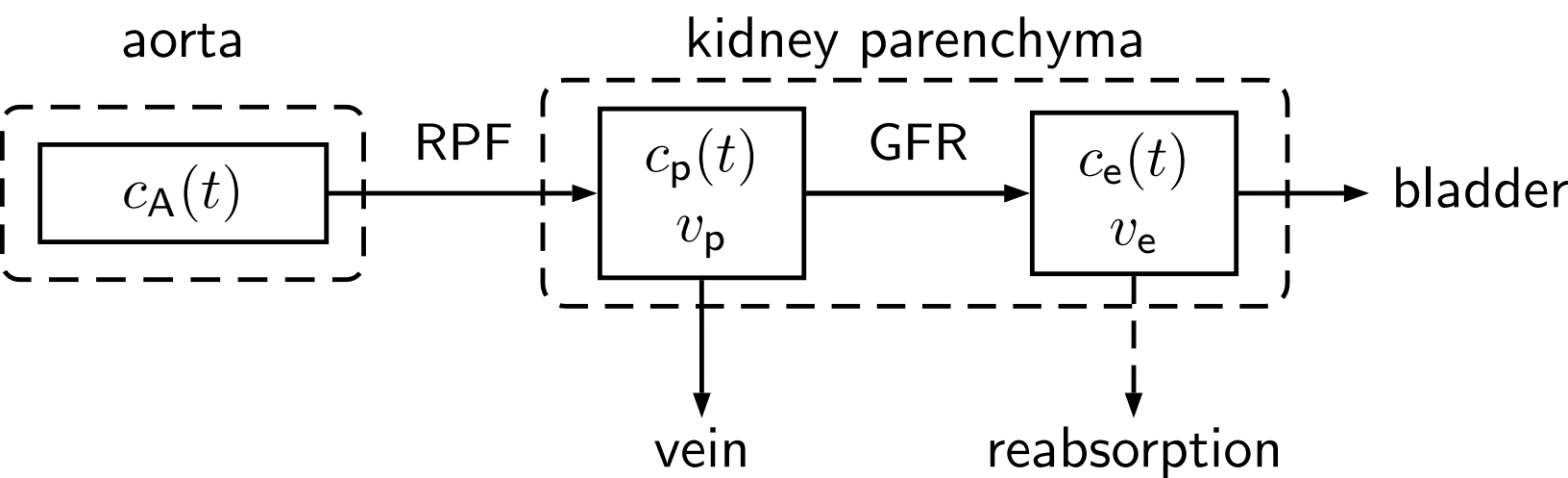


Figure 4

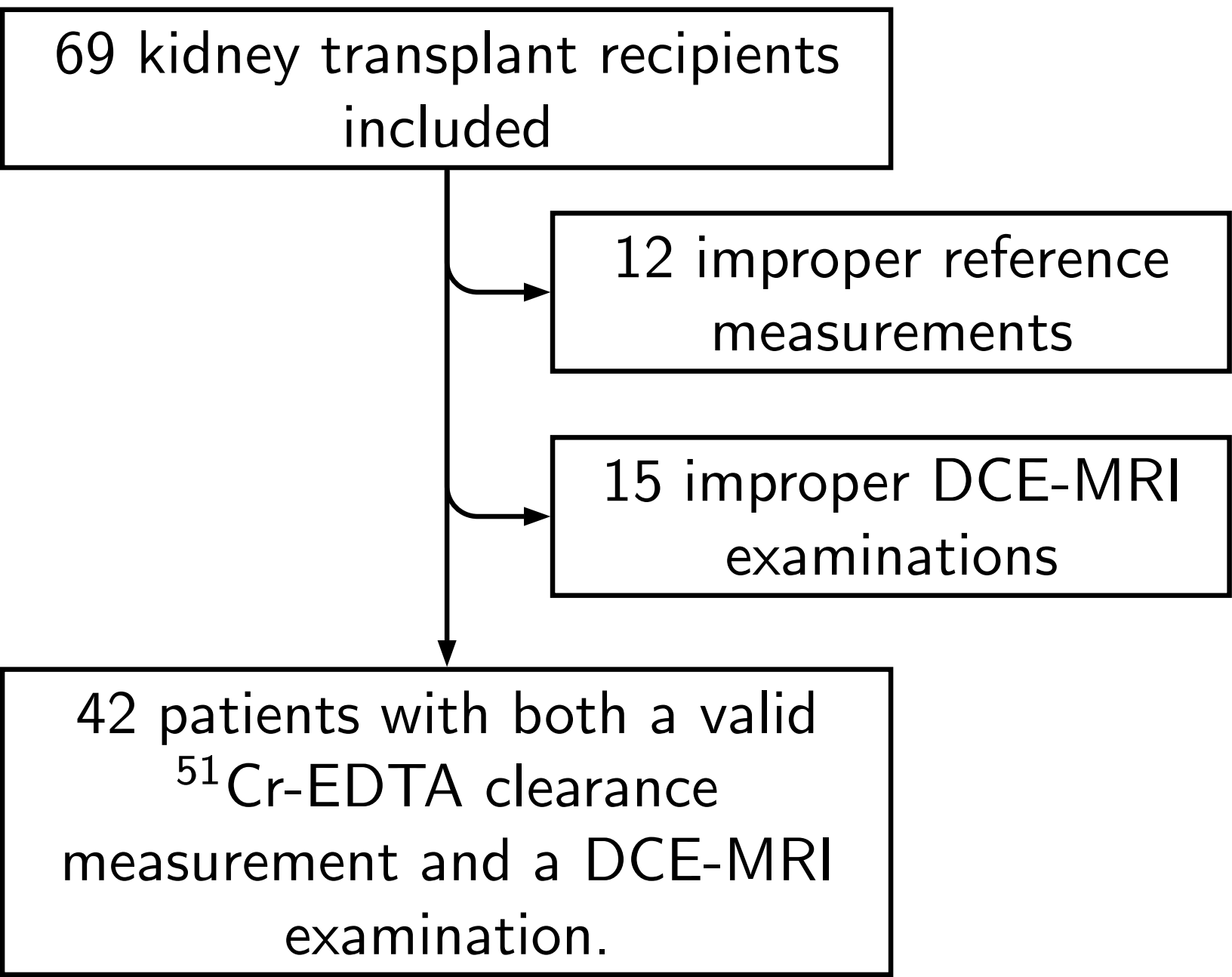


Figure 5

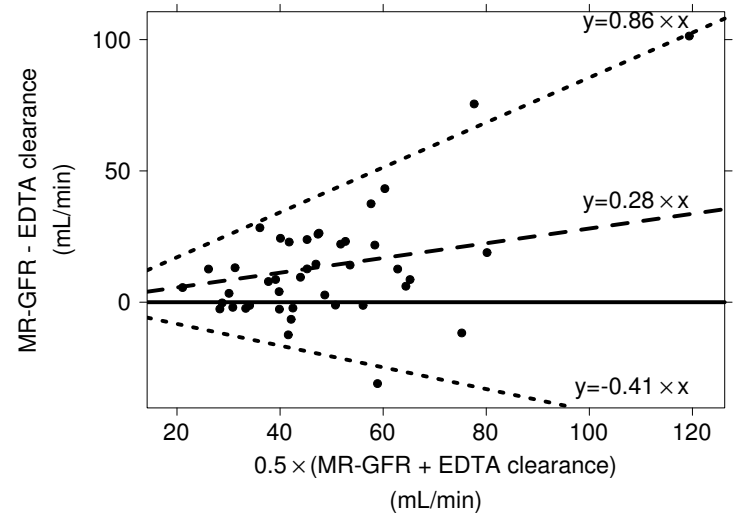
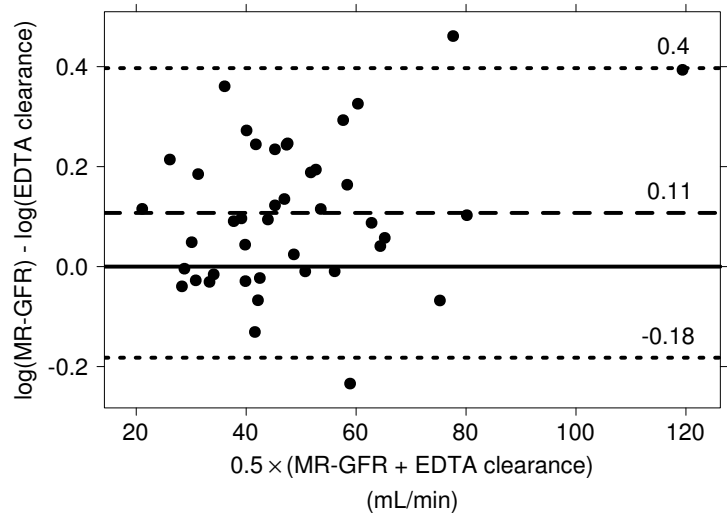
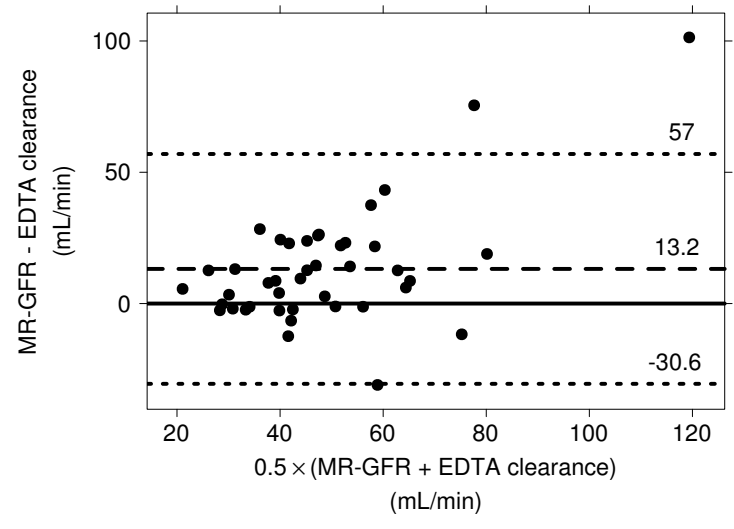
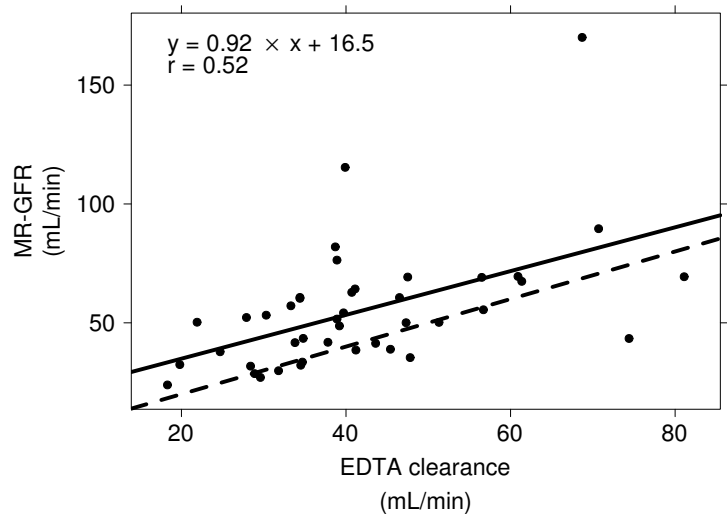
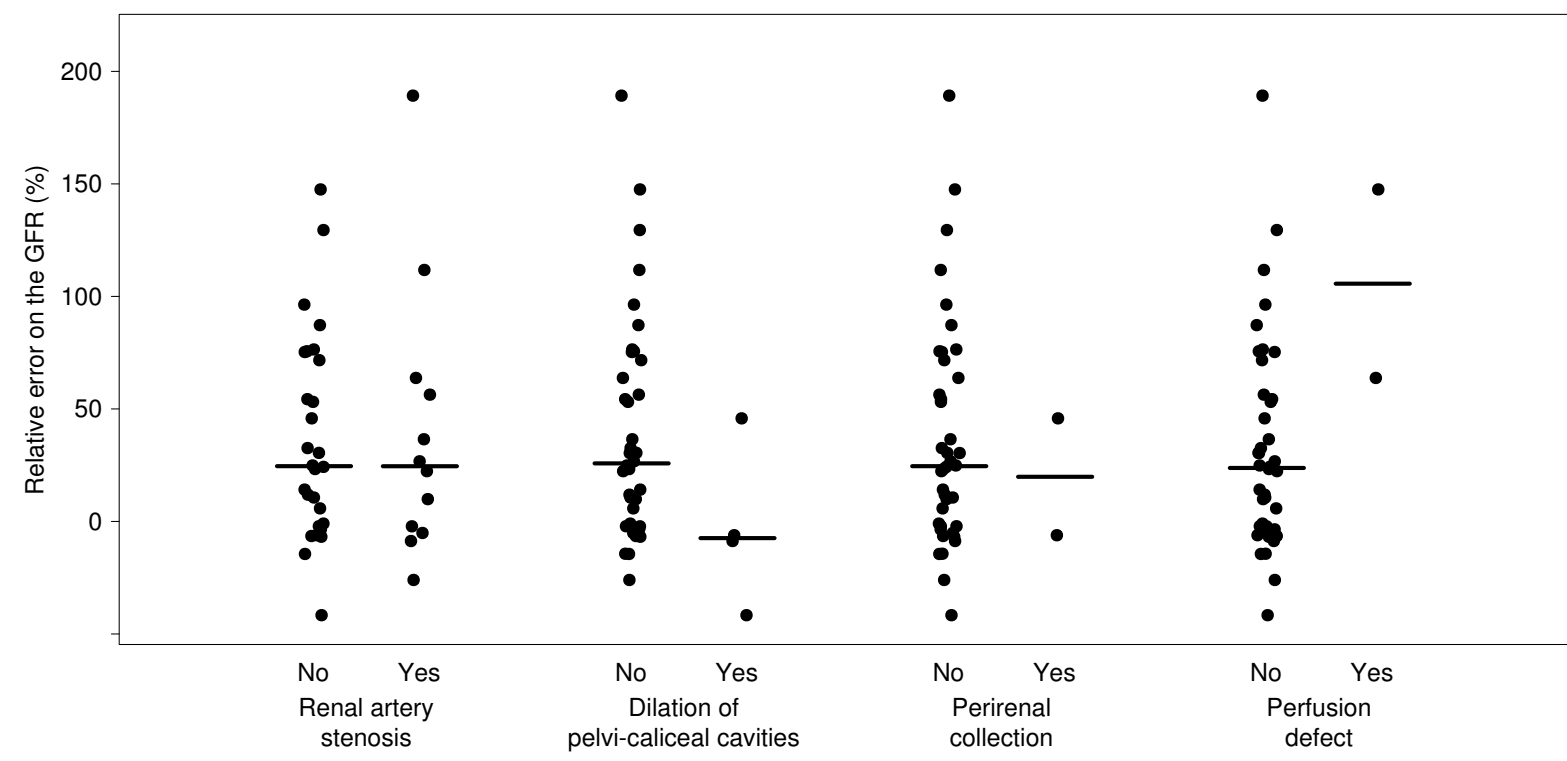
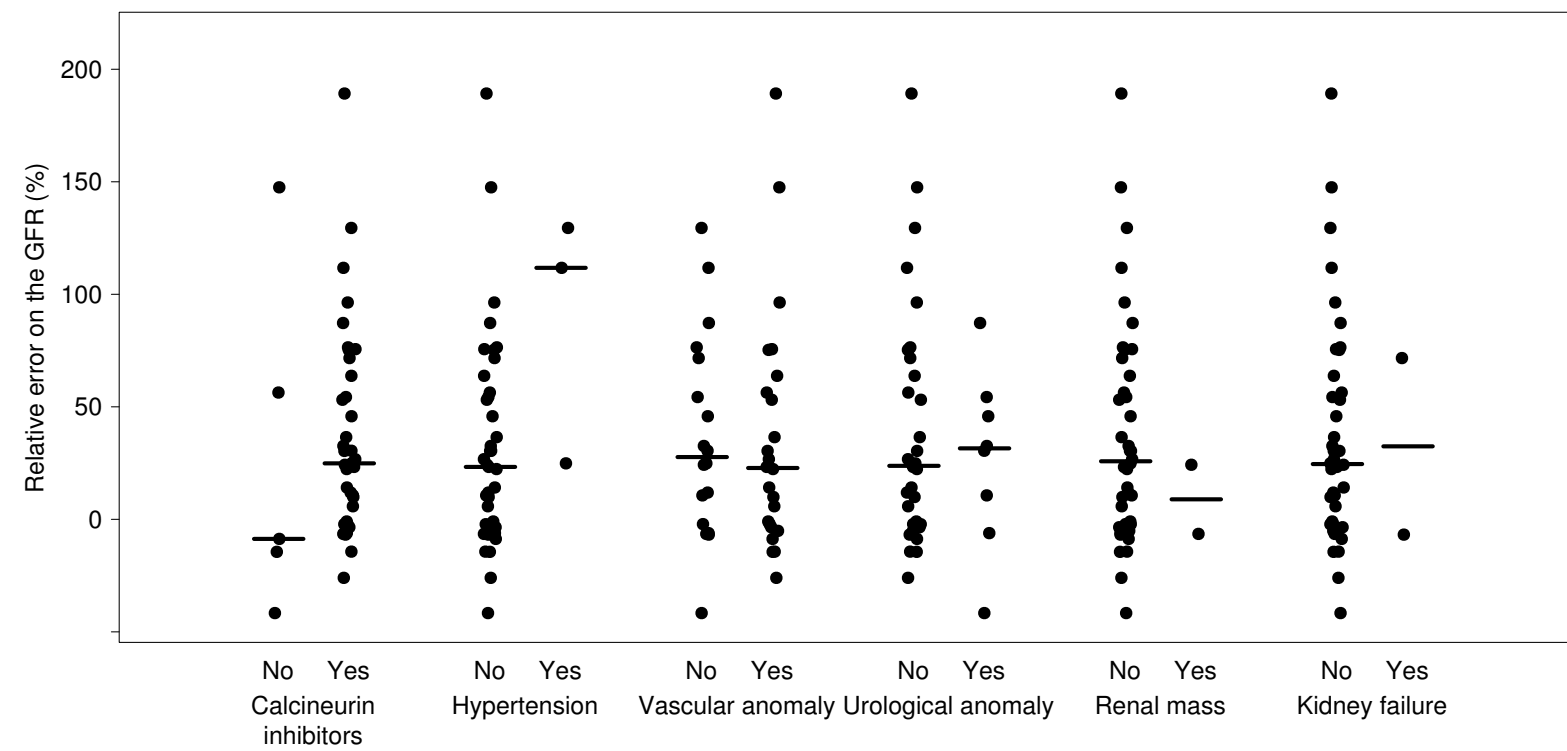


Figure 6



**Supplemental material**

[Click here to download Supplementary File\(s\): supplemental-material.docx](#)